AFRL-RY-WP-TR-2021-0182

A CRITICAL ASSESSMENT OF ELECTRON TRANSPORT THEORY

Revised Theory of Ionized Impurity Scattering- Phase 2

Daniel L. Rode

Pendragon Associates

AUGUST 2021

Final Report

DISTRIBUTION STATEMENT A. Approved for public release. Distribution is unlimited.

See additional restrictions described on inside pages

STINFO COPY

AIR FORCE RESEARCH LABORATORY
SENSORS DIRECTORATE
WRIGHT-PATTERSON AIR FORCE BASE, OH 45433-7320
AIR FORCE MATERIEL COMMAND
UNITED STATES AIR FORCE

NOTICE AND SIGNATURE PAGE

Using Government drawings, specifications, or other data included in this document for any purpose other than Government procurement does not in any way obligate the U.S. Government. The fact that the Government formulated or supplied the drawings, specifications, or other data does not license the holder or any other person or corporation; or convey any rights or permission to manufacture, use, or sell any patented invention that may relate to them.

This report was cleared for public release by the USAF 88th Air Base Wing (88 ABW) Public Affairs Office (PAO) and is available to the general public, including foreign nationals. Copies may be obtained from the Defense Technical Information Center (DTIC) (http://www.dtic.mil).

AFRL-RY-WP-TR-2021-0182 HAS BEEN REVIEWED AND IS APPROVED FOR PUBLICATION IN ACCORDANCE WITH ASSIGNED DISTRIBUTION STATEMENT.

//Signature//
JOHN S. CETNAR
Program Manager
Electronic Devices Branch
Aerospace Components & Subsystems Division

//Signature//
ROSS W. DETTMER, Chief
Electronic Devices Branch
Aerospace Components & Subsystems

//Signature//
LESTER C. LONG, Lt Col, USAF
Deputy
Aerospace Components & Subsystems Division
Sensors Directorate

This report is published in the interest of scientific and technical information exchange, and its publication does not constitute the Government's approval or disapproval of its ideas or findings.

*Disseminated copies will show "//Signature//" stamped or typed above the signature blocks.

REPORT DOCUMENTATION PAGE	*Form Approved* *OMB No. 0704-0188*

The public reporting burden for this collection of information is estimated to average 1 hour per response, including the time for reviewing instructions, searching existing data sources, searching existing data sources, gathering and maintaining the data needed, and completing and reviewing the collection of information. Send comments regarding this burden estimate or any other aspect of this collection of information, including suggestions for reducing this burden, to Department of Defense, Washington Headquarters Services, Directorate for Information Operations and Reports (0704-0188), 1215 Jefferson Davis Highway, Suite 1204, Arlington, VA 22202-4302. Respondents should be aware that notwithstanding any other provision of law, no person shall be subject to any penalty for failing to comply with a collection of information if it does not display a currently valid OMB control number. **PLEASE DO NOT RETURN YOUR FORM TO THE ABOVE ADDRESS**.

1. REPORT DATE *(DD-MM-YY)*	2. REPORT TYPE	3. DATES COVERED *(From - To)*
August 2021	Final	1 December 2020 – 1 December 2020

4. TITLE AND SUBTITLE
A CRITICAL ASSESSMENT OF ELECTRON TRANSPORT THEORY
Revised Theory of Ionized Impurity Scattering- Phase 2

5a. CONTRACT NUMBER
FA9550-20RXCOR046-RY

5b. GRANT NUMBER

5c. PROGRAM ELEMENT NUMBER
N/A

6. AUTHOR(S)
Daniel L. Rode

5d. PROJECT NUMBER
N/A

5e. TASK NUMBER
N/A

5f. WORK UNIT NUMBER
N/A

7. PERFORMING ORGANIZATION NAME(S) AND ADDRESS(ES)
Pendragon Associates
16400 Collins Avenue, Unit 2846
Sunny Isles Beach, Florida 33160

8. PERFORMING ORGANIZATION REPORT NUMBER

9. SPONSORING/MONITORING AGENCY NAME(S) AND ADDRESS(ES)

Air Force Research Laboratory Sensors Directorate Wright-Patterson Air Force Base, OH 45433-7320 Air Force Materiel Command United States Air Force	Air Force Office of Scientific Research Public Affairs (AFOSR) 875 North Randolph Street, Suite 325, Room 3112 Arlington, VA 22203

10. SPONSORING/MONITORING AGENCY ACRONYM(S)
AFRL/RYDD

11. SPONSORING/MONITORING AGENCY REPORT NUMBER(S)
AFRL-RY-WP-TR-2021-0182

12. DISTRIBUTION/AVAILABILITY STATEMENT
DISTRIBUTION STATEMENT A. Approved for public release. Distribution is unlimited.

13. SUPPLEMENTARY NOTES
PAO case number AFRL-2021-0823, Clearance Date 11 March 2021. Report contains color.

14. ABSTRACT
A revised theory is presented to account for electron scattering by ionized impurities in room temperature (300K) GaAs. The comparison between the revised theory and experiment shows agreement to within about 3 to 4%— far better than previous theories by Brooks-Herring and by Falicov-Cuevas. The revised theory also resolves a long-standing question regarding dopant compensation in GaAs. According to the revised theory, compensation does not appear to occur for Group VI dopants in GaAs. However, as expected, it does occur for an amphoteric dopant such as Si.

15. SUBJECT TERMS
degeneracy, electron mobility, electronic transport, semiconductor(s)

16. SECURITY CLASSIFICATION OF:			17. LIMITATION OF ABSTRACT:	18. NUMBER OF PAGES	19a. NAME OF RESPONSIBLE PERSON (Monitor)
a. REPORT	b. ABSTRACT	c. THIS PAGE			John Cetnar
Unclassified	Unclassified	Unclassified	SAR	19	19b. TELEPHONE NUMBER *(Include Area Code)* N/A

Table of Contents

Section **Page**

List of Figures ii
1 PHASE 2: A CRITICAL ASSESSMENT OF ELECTRON TRANSPORT THEORY—REVISED THEORY OF IONIZED IMPURITY SCATTERING 1
1.1 What Is Needed To Bring Theory and Experiment Into Agreement? 1
1.2 Electron Transport in GaAs 1
1.3 BH and FC Theories, and a Revised Theory of Electron Scattering 3
1.4 Dopant Compensation in GaAs 7
1.5 Electron Transport in GaN and Zinc Oxide (ZnO) 9
2 CONCLUSION 10
3 ACKNOWLEDGMENTS 11
APPENDIX 12
4 REFERENCES 13
LIST OF SYMBOLS, ABBREVIATIONS, AND ACRONYMS 14

DISTRIBUTION STATEMENT A. Approved for public release. Distribution is unlimited.

List of Figures

Figure **Page**

Figure 1: Electron mobility of GaAs at *T=300K* compiled by Sotoodeh[1] and by Stillman[2] *et al*. compared to BH theory (dashed curve) and FC theory (solid curve) 2
Figure 2: Same as Figure 1, showing the Degenerate Region Above $4x10^{17}/cc$ 3
Figure 3: Experimental Data Points are the same as in Figure 2 5
Figure 4: Experimental Data Points Same as Figure 1 6
Figure 5: Experimental Data Points (x) are by Mullin et al.. 6
Figure 6: Experimental Data Points are the same as shown in Figure 1... 7
Figure 7: Same as Figure 6 with the Addition of Data Points (x) for Si-doped Bulk-grown GaAs 8
Figure 8: Electron Hall Mobility Chart for Compensated GaAs at T = 300K and B = 10 kG... 9

DISTRIBUTION STATEMENT A. Approved for public release. Distribution is unlimited.

1 PHASE 2: A CRITICAL ASSESSMENT OF ELECTRON TRANSPORT THEORY—REVISED THEORY OF IONIZED IMPURITY SCATTERING

By Daniel L. Rode
Pendragon Associates

"To doubt everything or to believe everything are two equally convenient solutions; both dispense with the necessity of reflection." — Henri Poincaré

1.1 What Is Needed To Bring Theory and Experiment Into Agreement?

In Phase 1 of this work, it was shown that there is significant disagreement between theory and experiment regarding the electron mobility of heavily doped semiconductors, keeping in mind that the goal is to achieve agreement to within a few percent. Of particular concern is the widespread inclination to explain differences between theory and experiment by assuming dopant compensation by some arbitrary concentration of acceptor impurities, which in a few important cases is contrary to experiment, as pointed out in Phase 1. The present work, Phase 2, seeks to resolve this discrepancy.

In view of the fact that there exists a vast amount of experimental mobility data in the scientific literature, it is not surprising that there is a certain amount of spurious data, or data which are otherwise complicated by factors such as crystalline perfection, uniformity, substrate conduction, ohmic contacts, and so on. Therefore, with a focus on reliable data, the work in the next section is devoted primarily to a careful examination of perhaps the most thoroughly examined semiconductor of all – Gallium Arsenide (GaAs). However, the important wide-gap semiconductor Gallium Nitride (GaN) also receives some mention. This is followed by the introduction of a revised theory of electron scattering by ionized impurities.

In conclusion, to answer the question raised above, it appears certain that revision of the present theory of electron scattering by ionized impurities is necessary, and the work below shows a possible way to achieve this goal.

1.2 Electron Transport in GaAs

In the Phase 1 portion of this work, the experimental mobility of electrons in doped GaAs was presented (ref. Figure 11 therein)[1,2] as repeated below in Figure 1 and compared to theories by Brooks-Herring (BH)[3] and by Falicov-Cuevas (FC).[4] Copious additional experimental data on the 300K GaAs electron mobility can be found in the scientific literature.[5,6,7,8,9] The BH theory, insofar as it assumes a perfectly random spatial distribution of impurities, sets an upper bound to the theoretical mobility. However, although from a purely physical-vapor-deposition point of view such randomness might be expected, it is almost certain that this condition is not met experimentally. Indeed, there are experimental data contradicting it.[10,11]

DISTRIBUTION STATEMENT A. Approved for public release. Distribution is unlimited.

On the other hand, the assumption by FC of an exponential distribution seems to represent the opposite extreme, if by "exponential" these authors imply a Boltzmann probability distribution in equilibrium at some fictive temperature. Unfortunately, the authors do not elaborate, and they are unavailable for consultation. Thus, it is seen in Figure 1 that the curve for BH lies above the experimental data, and the curve for FC lies below the data when the electron concentration exceeds $1x10^{17}/cc$. Figure 2 emphasizes the more heavily doped region.

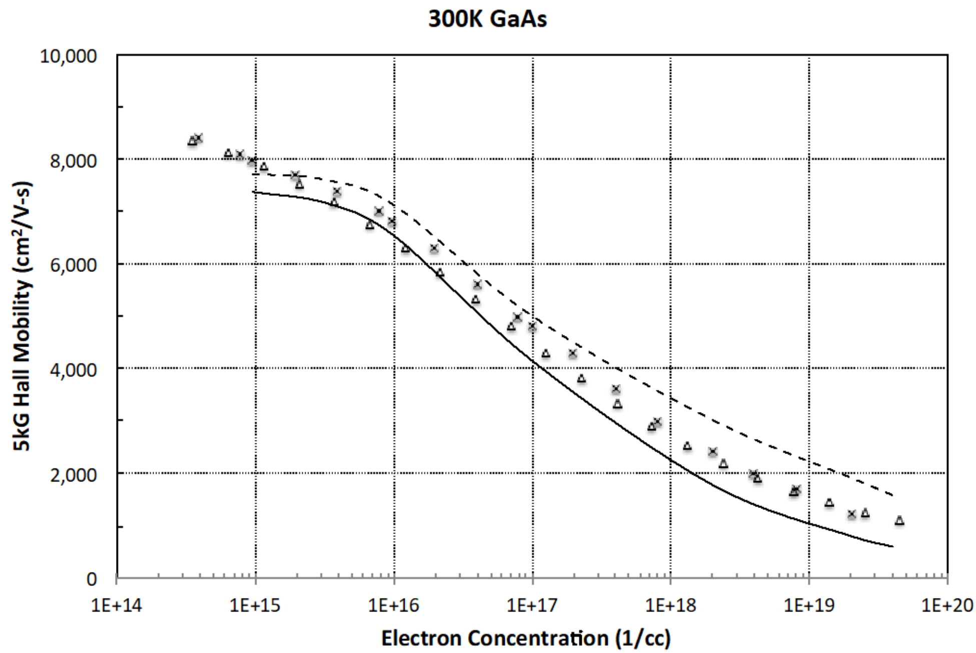

Figure 1: Electron mobility of GaAs at *T=300K* compiled by Sotoodeh[1] and by Stillman[2] *et al*. compared to BH theory (dashed curve) and FC theory (solid curve)
The assumed compensating acceptor concentration is 3.1x1015/cc. The effect of compensation is apparent below 1x1016/cc as the flattening of the curves.

DISTRIBUTION STATEMENT A. Approved for public release. Distribution is unlimited.

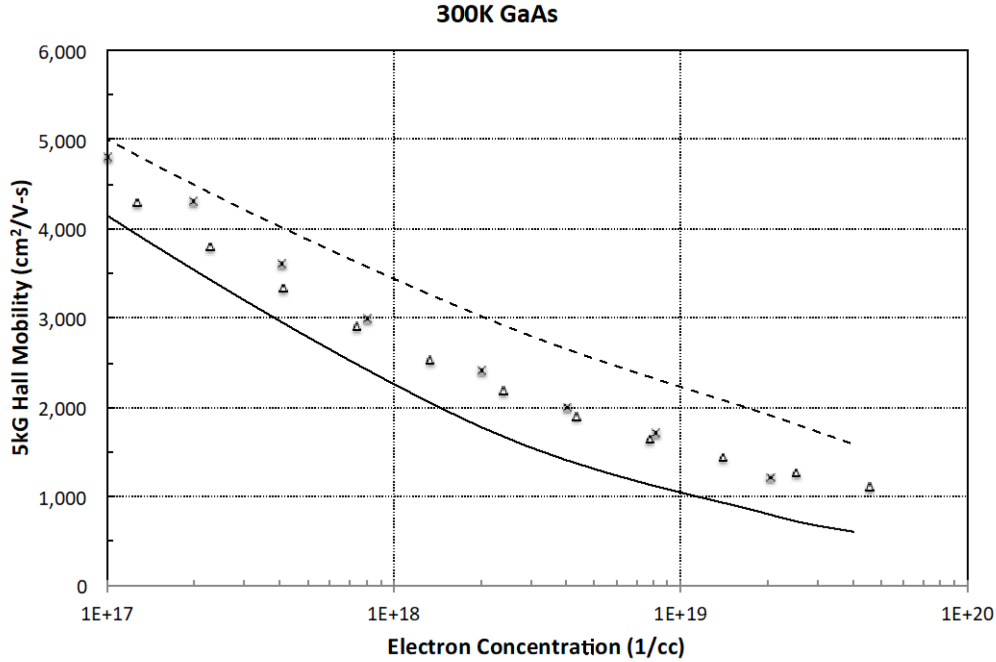

Figure 2: Same as Figure 1, showing the Degenerate Region Above 4x10^{17}/cc

The disagreement between BH and FC theory, and experiment is in the neighborhood of 30 to 40%. Therefore, it can be seen from Figure 2 that neither theory is acceptable to within the few percent accuracy desired.

1.3 BH and FC Theories, and a Revised Theory of Electron Scattering

Let us now proceed toward a remedy for this discrepancy. The scattering rate for conduction electrons can be expressed in terms of the momentum wave vector k and the ionized-impurity screening factor β aside from a pre-factor, which is constant with respect to k and β. For the BH theory, the scattering rate is[3.12]

$$\upsilon_{ii} = const. \cdot [D \cdot \ln(1 + 4k^2/\beta^2) - B]/k^3 \tag{1}$$

where

$$B = \frac{4k^2/\beta^2}{1+4k^2/\beta^2} + \frac{8\beta^2 + 16k^2}{\beta^2 + 4k^2} \cdot c^2 + \frac{3\beta^4 + 6\beta^2 k^2 - 8k^4}{(\beta^2 + 4k^2)k^2} \cdot c^4 \tag{2}$$

and

$$D = 1 + (2\beta^2 c^2/k^2) + (3\beta^4 c^4/4k^4) \tag{3}$$

The quantity c is a measure of wave function admixture, equal to zero for parabolic conduction bands, and rising to typically about 0.4 for degenerate doping conditions.[12] For the FC theory, the scattering rate is[4]

DISTRIBUTION STATEMENT A. Approved for public release. Distribution is unlimited.

$$\upsilon_{ii} = const. \cdot [D \cdot \ln(1 + 4k^2 / \beta^2) + B] / k^3 \quad (4)$$

Notice the plus sign in equation (eq.). 4 instead of the minus sign in eq. 1. This leads to significant differences for increasing electron concentrations. Eqs. 1 and 4 were used to calculate the curves drawn in Figure 1 and 2.

On the other hand, we find the following formulation gives satisfactory results for the case of GaAs at *300K*.[13]

$$\upsilon_{ii} = const. \cdot [D \cdot \ln(1 + 4k^2 / \beta^2) - B] / k^3 \quad (5)$$

where

$$B = \frac{k^2 / \beta^2}{1 + 4k^2 / \beta^2} + \frac{2\beta^2 + 4k^2}{\beta^2 + 4k^2} \cdot c^2 + \frac{3\beta^4 / 4 + 3\beta^2 k^2 / 2 - 2k^4}{(\beta^2 + 4k^2)k^2} \cdot c^4 \quad (6)$$

and

$$D = 1 + (2\beta^2 c^2 / k^2) + (3\beta^4 c^4 / 4k^4) \quad (7)$$

Note that eq. 5 is unchanged from eq. 1 and eq. 7 is unchanged from eq. 3, but eq. 6 is one-fourth of eq. 2.

This revision to the theory gives the result shown in Figure 3. The agreement over the range $n = 1x10^{17}/cc$ to $4x10^{19}/cc$ leaves little to be desired. For smaller electron concentrations, acceptor compensation comes into play, as shown in Figure 1. The triangular points are taken from a curve-fitting equation derived by Sotoodeh *et al.*[1] and it is perhaps questionable to extend it into the regime above $4x10^{19}/cc$. At that point, conduction in upper conduction band minima should come into play, but the theory does not incorporate these effects. Indeed, the data point by Stillman *et al.*[2] at $2x10^{19}/cc$ probably represents the upper limit that has been reached experimentally. The highest electron concentration point by Sotoodeh *et al.* is calculated from their empirical equation and may not exist experimentally. Thus, the mobility curves are shown dashed above $2x10^{19}/cc$ in the following section.

DISTRIBUTION STATEMENT A. Approved for public release. Distribution is unlimited.

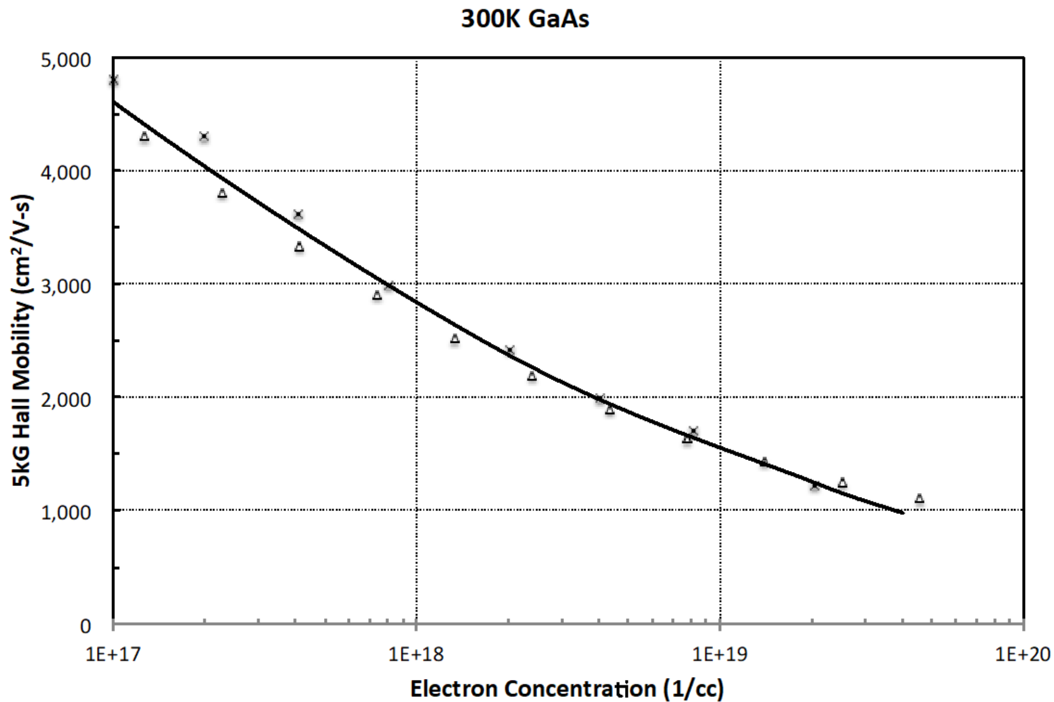

Figure 3: Experimental Data Points are the same as in Figure 2
The revised theory of eqs. 5-7 is used for the solid curve.

Figure 4 shows the same results for the entire electron concentration range used in Figure 1. The effects of acceptor impurity compensation are evident at the lower electron concentrations, and are expected to vary from sample to sample in uncorrelated fashion, so nothing further can be said on this point. The theoretical curves assume the compensating acceptor concentration is $2.8x10^{15}/cc$. Obviously, the revised theoretical curve (solid) represents the experimental data far more accurately.

Insofar as the experimental data shown in Figure 4 are for epitaxially grown GaAs, by vapor phase epitaxy (VPE) and liquid phase epitaxy (LPE), using various growth temperatures in the range of 650 to 850°C, it may be asked: "What is the effect of other crystal growth methods?" To this end, Mullin *et al.*[8] have reported electron mobility measurements on both vertically and horizontally grown bulk GaAs ingots where the growth temperature is 1238°C. Results for the group-VI donor dopants Selenium (Se) and Tellurium (Te) are shown in Figure 5. Since Se and Te reside on As sites as donors, they are not expected to be accompanied by dopant compensation, and this is confirmed by the results in Figure 5 above the $mid\text{-}10^{17}/cc$ electron concentration level.

DISTRIBUTION STATEMENT A. Approved for public release. Distribution is unlimited.

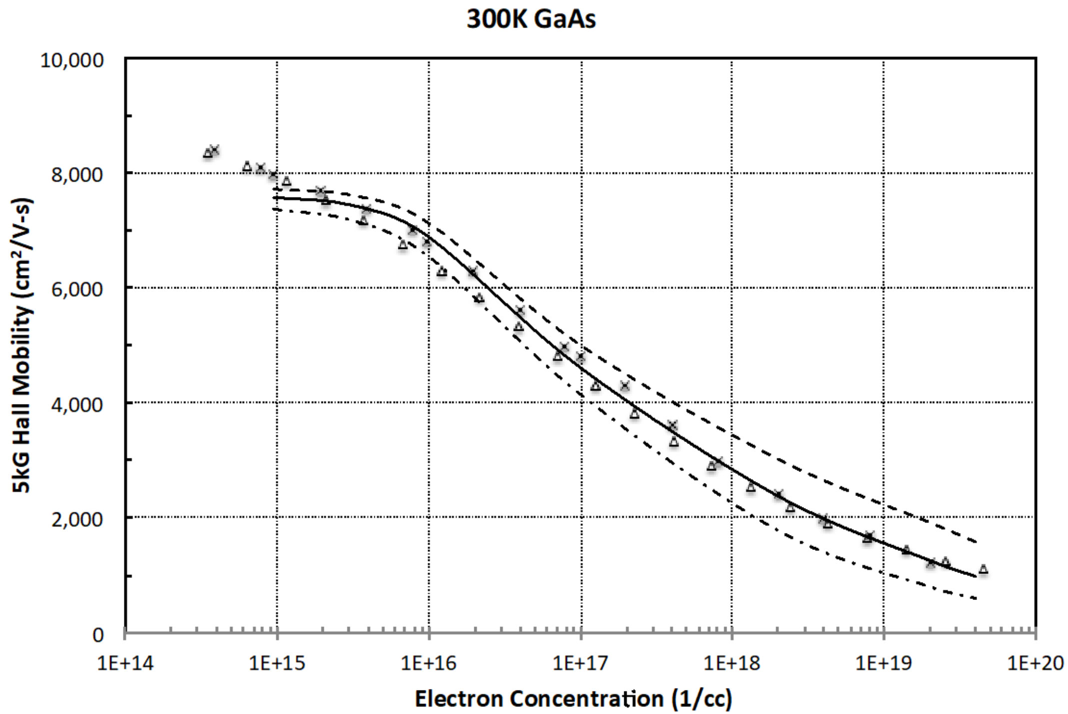

Figure 4: Experimental Data Points Same as Figure 1

BH and Falicov-Cuevas (FC) theory are upper and lower curves. The revised theory (eqs. 5-7) is shown as the solid curve.

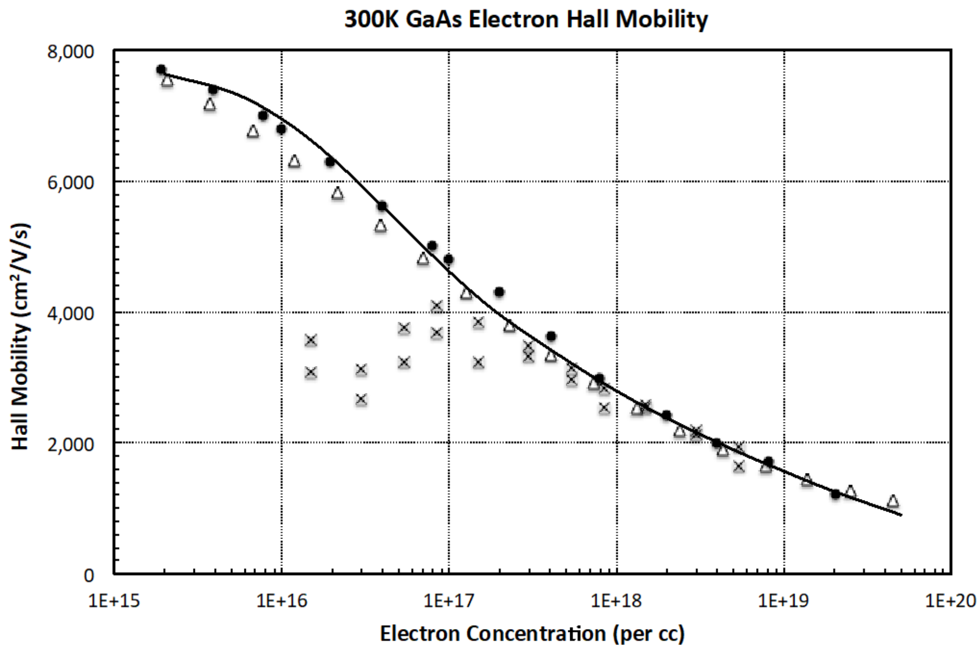

Figure 5: Experimental Data Points (x) are by Mullin et al

Revised theory is the solid curve, with acceptor concentration 2.8x10^{15}/cc

DISTRIBUTION STATEMENT A. Approved for public release. Distribution is unlimited.

For the smaller electron concentrations shown in Figure 5 compensation due to acceptors is to be expected, as observed. The derived acceptor concentration for the epitaxial material is in the *tens-of-parts-per-billion* range; for the bulk material it is in the *hundreds-of-parts-per-billion* range. Considering that the bulk material was grown in silica crucibles, and the epitaxial material was grown in hydrogen ambient in silica tubes, this is not surprising, compensation by C and Si impurities being expected.

1.4 Dopant Compensation in GaAs

However, this is not to say that dopant compensation cannot occur in GaAs and other materials. A convenient way to quantify this behavior is by use of a mobility chart, an example of which is shown in Figure 6. Here, the experimental data from Figure 1 are plotted along with curves from the revised theory for five different levels of dopant compensation, measured as the ratio of acceptor-to-donor concentration.

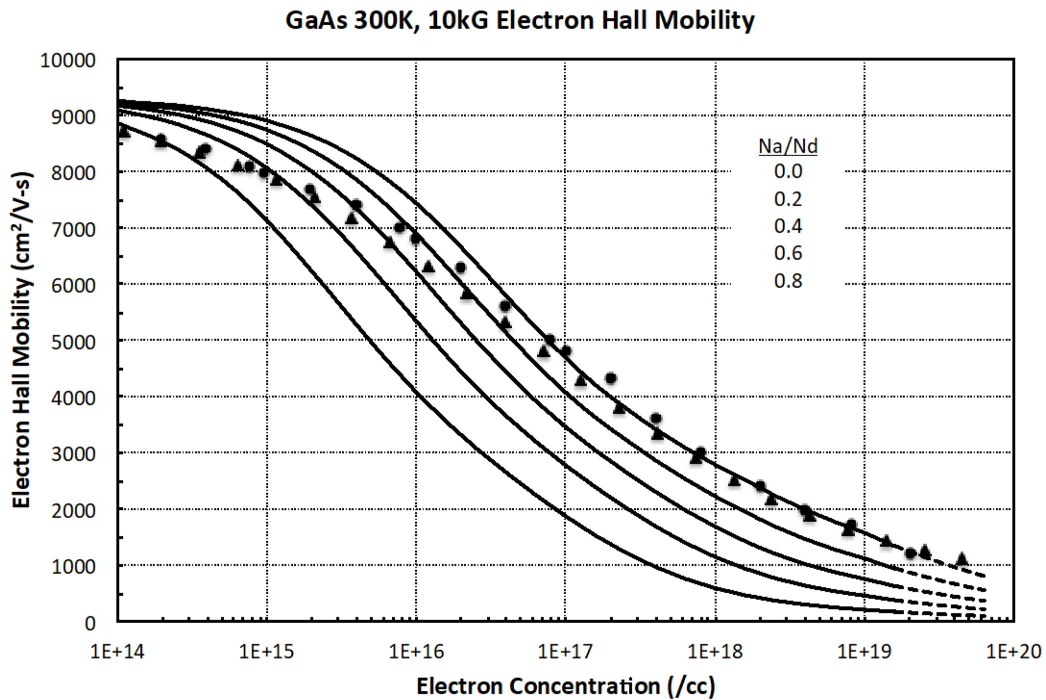

Figure 6: Experimental Data Points are the same as shown in Figure 1
The revised theory is used for the solid curves for five different compensation ratios.

For example, the datum shown at $2x10^{14}/cc$ in Figure 6 has a compensation ratio of 0.8 so that $N_d = 1x10^{15}/cc$ and $N_a = 8x10^{14}/cc$. Compensation is progressively negligible at larger electron concentrations. On the other hand, when an amphoteric dopant such as Si is used as a dopant in GaAs, compensation is to be expected at all doping levels. Si is predominantly a donor for growth temperatures above 830°C and predominantly an acceptor below 810°C. This circumstance is used industrially to manufacture annually billions of light emitting diode (LEDs) for opto-couplers and TV remote controls. This leads to the behavior shown in Figure 7 where the compensation ratio for bulk-grown, Si-

DISTRIBUTION STATEMENT A. Approved for public release. Distribution is unlimited.

doped GaAs exhibits a compensation ratio of 0.2. So, for example when $n = 2x10^{18}/cc$ one finds $N_d = 2.5x10^{18}/cc$ and $N_a = 5x10^{17}/cc$. This finding is also consistent with the suggestion that compensating acceptors in epitaxial GaAs arise predominantly from Si contamination due to interactions between hydrogen, HCl (for VPE), silica and the melt during crystal growth processes.[6,9]

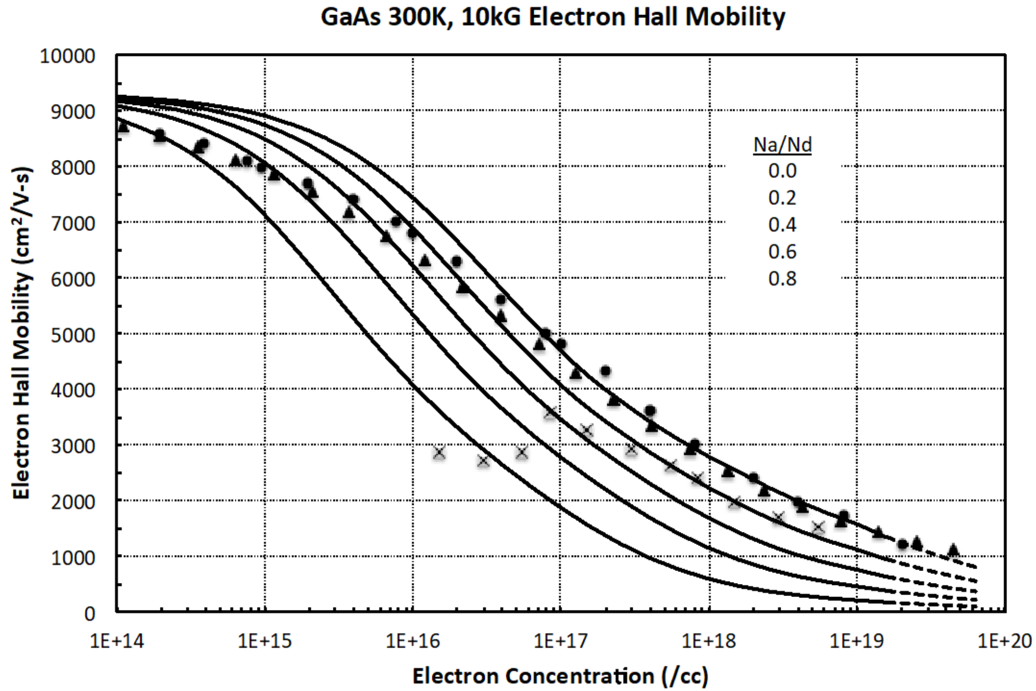

Figure 7: Same as Figure 6 with the Addition of Data Points (x) for Si-doped Bulk-grown GaAs

The revised theory gives a compensation ratio of 0.2 for the bulk-grown GaAs.

For the convenience of those wishing to use the 300K GaAs electron mobility chart to reduce experimental data, a clean copy is attached as Figure 8. The dashed portions of the curves follow from the discussion above in Section III. Conduction in higher lying conduction bands is expected to occur above $2x10^{19}/cc$ and this is not accounted for by the theory.

DISTRIBUTION STATEMENT A. Approved for public release. Distribution is unlimited.

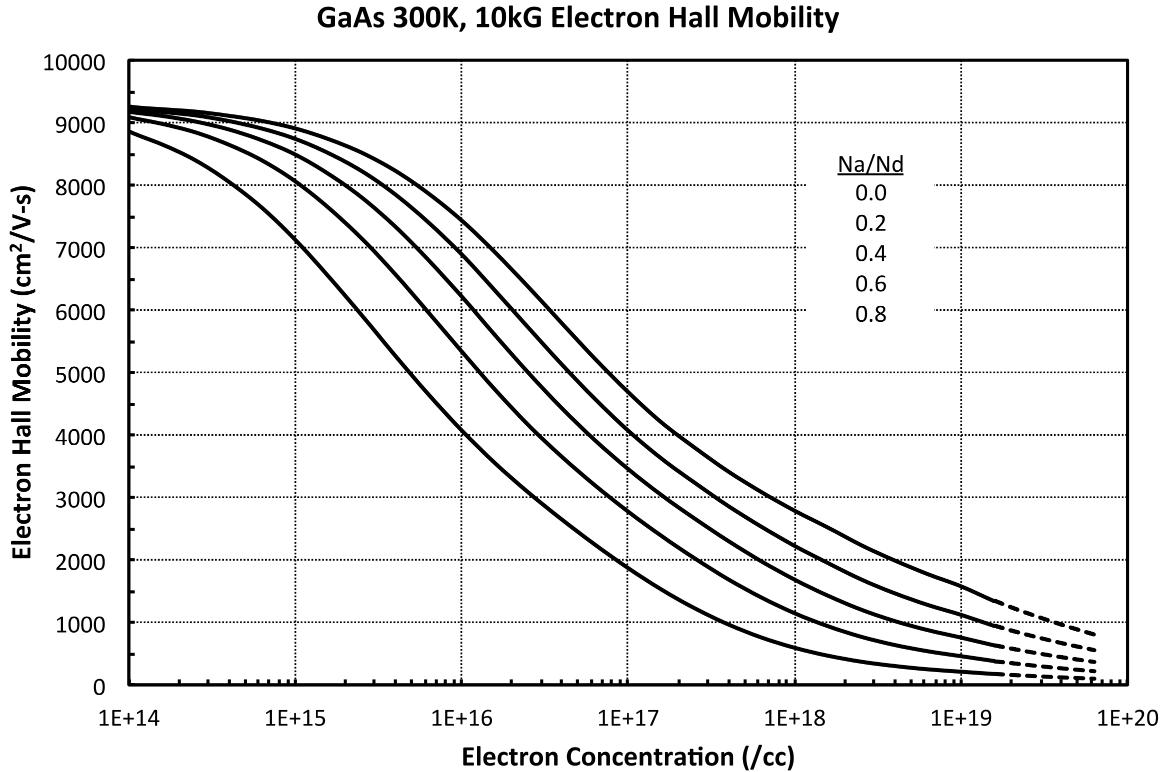

Figure 8: Electron Hall Mobility Chart for Compensated GaAs at T = 300K and B = 10 kG

1.5 Electron Transport in GaN and Zinc Oxide (ZnO)

Although the use of GaAs is commercially widespread, there is also great interest in the development of semiconductors with larger energy gaps, such as GaN and ZnO. These materials could potentially form the basis for new fields of high-power and high-temperature electronics and photonics. Hence, there is interest in the electron transport properties of these materials along the lines of the above analysis. Although it is not intended to go extensively into the question of GaN here, we can point to experimental work by Kim *et al.*[14] and theoretical work by Rode and Gaskill[15] which showed that agreement between theory and experiment can be obtained to within 2.5%. However, that work is limited to just two cases and clearly more work is needed at other doping levels and temperatures before conclusions can be drawn.

DISTRIBUTION STATEMENT A. Approved for public release. Distribution is unlimited.

2 CONCLUSION

The goal of Phase 1 of this work was to show that the previous theory of electron transport in semiconductors is no more accurate than about 30 to 40%, as shown in Figure 2. In the present part of the work, Phase 2, a revised theory is presented to account for electron scattering by ionized impurities, as given by eqs. 5 to 7. The comparison between the revised theory and experiment shown in Figure 3 shows agreement to within about 3 to 4%— far better than previous theory.

The revised theory also resolves a long-standing question regarding dopant compensation in GaAs.[5,6,7,8] According to the revised theory, compensation does not appear to occur for Group VI dopants in GaAs (see Figure 5). However, as expected, it does occur for an amphoteric dopant such as Si as shown Figure 7.

Finally, it is now possible to draw up an electron Hall mobility chart for 300K GaAs and this is presented as Figure 8.

Therefore, we conclude that a theory of electron transport, accurate to within a few percent, is now available — at least for GaAs at room temperature.

But what conclusions may be drawn regarding other materials and other temperatures? In a future Phase 3 of this work, GaN and degenerately Ga-doped ZnO will be examined in view of the revised theory. Thanks to very precise work carried out by AFRL on GZO, excellent experimental data are available, which have not previously been theoretically explained. This experimental work will allow a further rigorous test of the efficacy of the revised theory.

In conclusion, for the first time, it is with great satisfaction that we can point out the way to a historically accurate theory of electron transport in doped semiconductors in the form of eqs. 5 to 7.

DISTRIBUTION STATEMENT A. Approved for public release. Distribution is unlimited.

3 ACKNOWLEDGMENTS

Supported by the Air Force Office of Scientific Research under Project FA9550-20RXCOR046-RY. This work would not have been possible without encouragement and advice from John S. Cetnar. It is a pleasure to acknowledge helpful suggestions and discussions with David C. Look.

DISTRIBUTION STATEMENT A. Approved for public release. Distribution is unlimited.

APPENDIX

Theoretical calculations for this report were executed using an updated version of the computer program semiconductor electronic transport analysis (SETA). In order to get the accuracy required for high levels of degeneracy, the Fermi Level was calculated by three methods: a) from the Cetnar-Rode equation[16,17] (eq. 19 therein), b) from a bifilar iteration scheme[13], and c) from SETA itself, which is another iteration scheme. The calculations agree to within 0.1 meV, which is quite adequate for present purposes. The material parameters used for 300K GaAs calculations are the same as those in Rode[12] except energy gap, and are as follows. The effective-mass energy gap used below differs slightly from the optical-absorption energy gap as discussed by Rode[12] (see eq. 22 therein), but the effect of the difference on mobility is very small, typically about 0.2%.

GaAs:

low-frequency dielectric constant 12.91
high-frequency dielectric constant 10.91
optical phonon temperature 419K
elastic constant $1.4\text{x}10^{11}$ N/m^2
deformation potential 8.6 eV
piezoelectric coefficient 0.052
effective-mass energy gap 1.48 eV at 300K
effective mass 0.066m at 300K

DISTRIBUTION STATEMENT A. Approved for public release. Distribution is unlimited.

4 REFERENCES

1. M. Sotoodeh, A. H. Khalid, and A. A. Rezazadeh, J. Appl. Phys. **87** (2000) 2890.
2. M. R. Borzel and G. E. Stillman, *Properties of Gallium Arsenide*, (INSPEC, London, 1996) p. 106.
3. H. Brooks, Advan. Electron. Electron Phys. **7** (1955) 85, and C. Herring, unpublished.
4. L. M. Falicov and M. Cuevas, Phys. Rev. **164** (1967) 1025.
5. E. Veuhoff, M. Maier, K.-H. Bachem, and P. Balk, J. Crystal Growth **53** (1981) 598.
6. E. Kuphal, J. Crystal Growth **54** (1981) 117.
7. D. A. Anderson and N. Apsley, J. Appl. Phys. **58** (1985) 3059.
8. J. B. Mullin, A. Royle, and S. Benn, J. Crystal Growth **50** (1980) 625.
9. DiLorenzo, J. Crystal Growth **17** (1972) 189.
10. L. H. Ouyang, D. L. Rode, T. Zulkifli, Barbara Abraham-Shrauner, N. Lewis, and M. R. Freeman, J. Appl. Phys. 91, 3459 (1 March 2002).
11. B. Fischer, E. Bauser, P. A. Sullivan, and D. L. Rode, Appl. Phys. Letters **33** (1978) 78.
12. D. L. Rode, *Semiconductors and Semimetals* **15** (Academic Press, New York, 1975) Ch. 1.
13. D. L. Rode, unpublished work.
14. J. G. Kim, A. C. Frenkel, H. Liu, and R. M. Park, Appl. Phys. Letters **65** (1994) 91.
15. D. L. Rode and D. K. Gaskill, Appl. Phys. Letters **66** (1995) 1972.
16. J. S. Cetnar and D. L. Rode, "Fermi Level and Electrostatic Screening Length in Degenerate Semiconductors and Metal Alloys", 60th Annual EMC, Santa Barbara, CA (2018).
17. J. S. Cetnar and D. L. Rode, Journal of Electronic Materials **48**, 3399 (2019).

DISTRIBUTION STATEMENT A. Approved for public release. Distribution is unlimited.

LIST OF SYMBOLS, ABBREVIATIONS, AND ACRONYMS

ACRONYM	DESCRIPTION
AFRL	Air Force Research Laboratory
BH	Brook-Herring
Eq	Equation
FC	Falicov-Cuevas
GaAs	Gallium Arsenide
GaN	Gallium Nitride
GZO	Gallium Zinc Oxide
LED	Light Emitting Diode
LPE	Liquid Phase Epitaxy
Se	Selenium
SETA	Semiconductor Electronic Transport Analysis
Te	Tellurium
TV	Television
VPE	Vapor Phase Epitaxy
ZnO	Zinc Oxide

DISTRIBUTION STATEMENT A. Approved for public release. Distribution is unlimited.